HHS Public Access

Author manuscript

Mucosal Immunol. Author manuscript; available in PMC 2014 November 01.

Published in final edited form as:

Mucosal Immunol. 2014 May ; 7(3): 501–510. doi:10.1038/mi.2013.67.

Lung Niches for the Generation and Maintenance of Tissue-resident Memory T cells

D. L. Turner[1,2], **K. L. Bickham**[1,2], **J. J. T. Thome**[1,3], **C. Y. Kim**[4], **F. D'Ovidio**[4], **E. J. Wherry**[5], and **D. L. Farber**[1,4]

[1]Columbia Center for Translational Immunology, Columbia University Medical Center, New York, NY 10032., Columbia University Medical Center, New York, NY 10032

[2]Department of Medicine, Columbia University Medical Center, New York, NY 10032., Columbia University Medical Center, New York, NY 10032

[3]Department of Microbiology and Immunology, Columbia University Medical Center, New York, NY 10032., Columbia University Medical Center, New York, NY 10032

[4]Department of Surgery, Columbia University Medical Center, New York, NY 10032., Columbia University Medical Center, New York, NY 10032

[5]Department of Microbiology, University of Pennsylvania School of Medicine, Philadelphia, PA 19104

Abstract

The extent to which tissue-specific viral infections generate memory T cells specifically adapted to and maintained within the target infection site is unknown. Here, we show that respiratory virus-specific memory T cells in mice and humans are generated and maintained in compartmentalized niches in lungs, distinct from populations in lymphoid tissue or circulation. Using a polyclonal mouse model of influenza infection combined with an *in vivo* antibody labeling approach and confocal imaging, we identify a spatially distinct niche in the lung where influenza-specific T cell responses are expanded and maintained long term as tissue resident memory (T_{RM}) CD4 and CD8 T cells. Lung T_{RM} are further distinguished from circulating memory subsets in lung and spleen based on CD69 expression and persistence independent of lymphoid stores. In humans, influenza-specific T cells are enriched within the lung T_{RM} subset, while memory CD8 T cells specific for the systemic virus CMV are distributed in both lung and spleen, suggesting that the site of infection affects T_{RM} generation. Our findings reveal a precise spatial organization to virus-specific T cell memory, determined by the site of the initial infection, with important implications for the development of targeted vaccination and strategies to boost immunity at appropriate tissue sites.

To whom correspondence should be addressed: Donna L. Farber: Columbia Center for Translational Immunology, Columbia University Medical Center, 650 W 168th Street, New York, NY 10032; phone: 212-305-6030; FAX: 646-426-0019; df2396@cumc.columbia.edu.

INTRODUCTION

Respiratory infection generates T cell responses detectable in lymphoid tissue and lung. The relative contribution of circulating and site-specific immunity to longterm memory responses and the mechanisms which govern their generation and maintenance remain poorly understood in both mouse models and humans. In the case of respiratory viruses such as influenza, infection is confined to the lung, yet systemic immune responses are generated--including flu-specific antibodies in serum and lung [1, 2], and virus-specific memory T cells in multiple tissues including lungs, spleen, lymph nodes, and liver [3–5]. Because memory CD4 and CD8 T cells can be cross-reactive to multiple flu strains[6, 7], and can provide heterotypic protection in mouse models, they are key targets for promoting successful respiratory immunity. Defining the role of anatomic localization in the development and maintenance of anti-viral T cell memory responses in influenza and other viruses can therefore alter the way in which we design, monitor and target vaccines.

Heterogeneous distribution of virus-specific T cells in lymphoid and non-lymphoid sites occurs following infection with respiratory or systemic viruses [8–11], suggesting that maintaining diversity in the memory T cell population may be advantageous for protection. However, the extent to which an initial immune response to influenza in the lung remains compartmentalized is not known, and has been difficult to establish whether a particular T cell in the lung recirculates or remains localized. Recent studies suggest that subsets of memory T cells are retained at specific sites as tissue-resident memory T cells or T_{RM}, and may confer an effective *in situ* first line of defense to tissue-specific infections[12–14]. CD8 T_{RM} have been described in the skin[15], brain[16], gut[17], vaginal mucosae[18, 19], and lung[20], while CD4 T_{RM} have not been as well-defined. We recently identified a subset of TCR-transgenic, influenza hemagglutinin (HA)-specific lung memory CD4 T cells that were specifically retained in the lung and did not circulate to other sites [21]. These lung resident memory CD4 T cells mediated optimal protection to influenza infection, while spleen-derived HA-specific memory CD4 T cells did not confer significant protection, despite their migration to the lung [21]. Together, these findings suggested that lung T_{RM} may occupy a distinct compartment in the lung compared to spleen memory T cells which could circulate to multiple tissue sites. Whether T_{RM} are generated distinct from circulating populations or derive from lymphoid progenitors is not known.

In this study, we investigated the generation, maintenance and localization of influenza-specific memory T cells *in vivo* and *in situ* in a polyclonal mouse model and in humans to address the hypothesis that the respiratory viruses generate specific memory T cell subsets that remain compartmentalized in the lung. Using an intravenous antibody labeling approach to differentiate between resident and circulatory T cells in the lung following influenza infection, we identified subsets of phenotypically distinct memory CD4 and CD8 T cells, which segregate within specific lung niches near the airways and in bronchovascular bundles. T cells within this niche were enriched for influenza-specific CD4 and CD8 T cells, expressed phenotypic markers associated with T_{RM}, including CD69, CD11a, and CD103, and were maintained long term after viral clearance, independent of replenishment from lymphoid stores. Importantly, in humans, influenza-specific CD8 T cells were enriched within the lung T_{RM} subset, while memory CD8 T cells specific for the systemic virus CMV

persisted as circulating populations in lung and spleen. Together, our results establish that T cell memory to respiratory viruses is generated and maintained in a spatially compartmentalized niche in the lung, creating organized foci of influenza-specific immune cells at the sites of pathogen entry.

RESULTS

Influenza infection alters the distribution and accessibility of CD4 T cells in the lung

Previous studies have analyzed tissue distribution and residence of virus-specific T cells using T cell receptor (TCR)-transgenic T cells[15, 18, 21, 22]. Here, we assessed how tissue residence and location influenced the development of influenza-specific memory T cells in unmanipulated, polyclonal mice as a more physiologically relevant system. We used an *in vivo* antibody labeling approach to differentiate cells in circulation and in tissues, in which fluorescently-coupled anti-CD4 antibody (IV anti-CD4) is administered intravenously to mice 10 minutes prior to lung tissue perfusion and harvest. Using IV anti-CD4, T cells accessible to circulation bind fluorescent Ab, while those embedded in the tissues and inaccessible to circulation are protected from labeling. We administered IV anti-CD4 to naïve and flu-infected BALB/c or C57BL/6 (B6) mice at different timepoints following infection to distinguish between T cells accessible to circulation that become labeled with antibody *in vivo* (“Labeled” subset) versus those within tissues which are protected from antibody labeling (“Protected” subset).

The kinetics of CD4 T cell recruitment and maintenance in the lung was assessed in naïve and flu-infected mice following IV anti-CD4 administration. In peripheral blood of naive and infected mice, the vast majority (>98%) of CD4 T cells were labeled following IV anti-CD4 infusion (Supplementary Figure 1s), indicating the efficiency of *in vivo* antibody binding of circulating T cells. In the lungs of naïve or mock-infected mice, >90% of CD4 T cells were labeled, with only a small fraction (< 10%) of total CD4 T cells protected from labeling (Figure 1a and b). Following intranasal infection with influenza virus, the proportion of protected lung CD4 T cells increased dramatically, comprising >25% of total lung CD4 T cells as early as 3 days post-infection, peaking at 60–70% of lung CD4 T cells at day 10 p.i., and remaining elevated for up to 3 weeks p.i., with concomitant reductions in the proportion of labeled CD4 T cells at these timepoints (Figure 1a and b). The elevated proportion of protected CD4 T cells in the lung during acute influenza infection was likewise reflected in a 3–5-fold increase in the absolute number of protected CD4 T cells between day 3 and 10 post-infection, and this number remained high up to three weeks post-infection (Figure 1c). At later times post-infection, when virus is cleared and viral antigens are no longer presented (≥day 28), the frequency of protected cells was reduced to a range of 20–40% (Figure 1a and b), which was stably maintained >120 days post-infection (Figure 1d). The absolute number of protected memory CD4 T cells at these later timepoints from 1–4 months post-infection was reduced compared to acute infection, but significantly increased compared to numbers in naïve mice (Figure 1c, e). These long-term protected T cells in the lung were not found significantly in bronchiolar lavage fluid (BAL), (Supplemental Figure 2s), further indicating that they are within the lung tissue.

Intravenous antibody labeling also revealed subsets of labeled and protected CD4 T cells in the spleen (Supplemental Figure 1s), similar to findings with splenic CD8 T cells[20], and corresponding to T cells in the red pulp and inside follicles, respectively ([20] and data not shown). The frequency of protected and labeled CD4 T cells in spleen was not appreciably altered during the course of influenza infection (Supplementary Figure 1s), indicating that the increase in protected T cells due to respiratory virus infection is specific to the lung. Therefore, quantitation of CD4 T cells during infection in a precise spatial location of the lung—defined here as the protected region-- reveals the kinetics and magnitude of a primary T cell response to infection, with an initial period of expansion/recruitment peaking between day 10–14 pi, followed by a contraction phase with a stable population of memory T cells maintained after viral clearance.

In vivo labeling defines phenotypic and functional subsets of CD4 T cells in naïve and flu-infected lungs

We then assessed whether labeled and protected T cells comprised distinct phenotypic and functional subsets. Total lung CD4 T cells from uninfected mice exhibited a predominant naive phenotype, and the majority of these naïve T cells were labeled (Figure 2a, top row), consistent with naïve T cells circulating through lung. During acute influenza infection (day 10 pi), the majority of total lung CD4 T cells exhibit an effector-like or effector-memory (T_{EM}) phenotype (CD44hi/CD62Llo); while effector cells are found in both labeled and protected subsets, all protected T cells were effector cells, and the small fraction of naïve T cells was exclusively in the labeled fraction (Figure 2a, middle row, and 2b). After viral clearance, total lung CD4 T cells comprised both naïve and T_{EM} cells, with naïve T cells exclusively within the labeled subset and protected cells predominantly T_{EM} CD4 T cells (Figure 2a, bottom row, and 2b). These results indicate that *in vivo* labeling can distinguish between two functionally distinct T cell subsets in the lung: naïve T cells that are readily accessible to circulation, and effector and T_{EM} CD4 T cells which are protected from IV anti-CD4 and in a circulation-inaccessible zone.

The early T cell activation marker CD69 was upregulated exclusively in the protected memory CD4 T cell subset in the lung, while labeled memory and naïve subsets were predominantly CD69-negative in the lung (Figure 2c) and spleen (data not shown). During the course of influenza infection, the frequency of CD69-expressing protected memory CD4 T cells fluctuated early after infection (day 3 p.i., Figure 2c), likely indicating the influx of effector cells which can downregulate this early activation marker. After viral clearance, protected T_{EM} were $CD69^{+}$ and $CD11a^{hi}$ (Figure 2c)—phenotypic properties of resident memory T cells (T_{RM}) in mucosal sites [15, 16, 21]. When taken together, the protected subsets bear phenotypic markers of lung T_{RM}, while the labeled subset comprises both circulating T_{EM} and naïve T cells.

Anatomical localization of labeled and protected CD4 T cells in distinct niches of the lung

We hypothesized that the protected and labeled CD4 T cell subsets occupy distinct anatomical niches within lung tissue. We used confocal microscopy to determine the distribution of the labeled and protected memory CD4 T cells in thick sections of the lung after *in vivo* labeling of naïve and flu-infected mice (Figure 3). Labeled CD4 T cells were

directly stained *in vivo* and appear blue or blue-violet, and protected CD4 T cells were revealed by *ex vivo* staining with a non-overlapping anti-CD4 antibody and appear red. For visualization of lung tissue structures, we used fluorescently-conjugated ECL lectin[23] which bind Type I alveolar epithelial cells and/or anti-collagen I antibodies which bind columnar epithelial cells around airways (see methods). In lungs of naïve mice, labeled CD4 T cells (blue) localize within the walls of the alveoli (Figure 3a and Supplementary Figure 3s-a), while protected lymphocytes (red) are only sparsely represented (Figure 3a). During acute infection (day 5 p.i.), however, there was a large increase in the numbers and appearance of protected cells which localized in large clusters around airways (Figure 3b), while labeled T cells were not significantly observed (Figure 3b, left). Protected CD4 T cells in acutely infected lungs filled the expanded space between the airways and lung parenchyma (Figure 3b), and likely represent effector cells. After viral clearance (3–4weeks p.i.), both protected and labeled cells can be fully visualized (Figure 3c, left), but occupy distinct spatial locations within the tissue: Protected memory CD4 T cells were observed in clusters in the narrow space around airways and near pulmonary vessels that make up bronchovascular bundles, while labeled CD4 T cells were distributed throughout the lung parenchyma and near alveolar walls and did not form clusters (Figure 3c and d; Supplementary Figure 3s-b). The persistence of protected CD4 T cells in the vicinity of airways is further shown in lung sections stained with anti-collagen antibodies without the alveolar staining (Figure 3d), and we did not observe them around minor blood vessels not associated with airways. These results therefore establish that protected T cells occupy a spatially distinct niche of the lung in a region near the site of antigen entry into the lung via airways.

We further examined whether the protected memory CD4 T cells persisting near the lung airways also upregulate CD69 *in situ*. In lungs of naïve mice, there were few $CD69^+$ CD4 T cells detected; however, in “flu-memory” mice 3–4 weeks post-infection, CD69 staining co-localized with CD4 T cells in clusters near the airways and radiating outwards (Figure 4). Taken together, these results demonstrate a spatial segregation of $CD69^+$ lung CD4 T_{RM} clustered in the vicinity of the airways.

Biased distribution of Influenza-specific memory T cells within lung T_{RM}

We examined whether polyclonal lung CD4 T_{RM} from flu-memory mice were enriched for influenza specificities, by stimulating lung CD4 T cells following IV anti-CD4 infusion, with uninfected or flu-infected APCs, and measuring influenza-specific IFN-γ secretion. In all cases, flu-specific IFN-γ secretion was detected predominantly by protected lung CD4 T_{RM}, and exceeded by 10-fold the frequency of flu-specific IFN-γ production by labeled lung memory CD4 T cells and by splenic CD4 T cells (Figure 5a). Interestingly, in the spleen, there was no bias in the distribution of flu-specific cells among protected and labeled CD4 T cell subsets, further establishing that segregation of flu-specific memory CD4 T cells into a spatial niche occurred only at the site of infection in the lungs. Moreover, protected lung T_{RM} CD4 T cells also responded to influenza challenge *in vivo*, while the labeled subset did not exhibit a significant recall response (Supplementary Figure 4s), indicating that lung T_{RM} are the early responders *in vivo*.

Using a similar IV Ab labeling approach, we investigated the distribution of CD8 T cells in different lung niches after influenza infection. In lungs of naïve or mock-infected mice, the vast majority (>90%) of lung CD8 T cells were labeled by IV Ab (Figure 5b, left), similar to CD4 T cells in naïve lungs. In flu-memory mice (>40 days post-infection) however, >70% of lung CD8 T cells were protected from IV anti-CD8. Moreover, the protected CD8 T cell subset in the lung contained a significantly higher proportion of flu-specific memory CD8 T cells (3–4 fold greater) compared to labeled lung T cells (Figure 5b), with the biased distribution of Flu-specific CD8 T cells in the protected niche maintained >120 days post-infection (Supplementary Figure 5s). By contrast, the overall percentage of flu tetramer-positive (Tet^+) cells in the spleen was significantly lower than in the protected lung niche and there was no difference in their frequency in protected and labeled fractions of splenic CD8 T cells (Figure 5b). In terms of absolute numbers, there were greater overall numbers of Tet^+ cells in the spleen compared to the protected lung niche due to its increased cellularity-- of the total numbers of Tet^+ CD8 T cells recovered from lymphoid and lung tissue, two-thirds were found in the spleen and one-third in the protected lung niche (Figure 5c).

Consistent with our results with CD4 T cells, Tet^+ flu-specific protected CD8 T cells were predominantly $CD69^+$ while Tet^+ cells among the labeled lung subset were CD69lo, as were all Tet^+ memory CD8 T cells in the spleen (Figure 5d). Expression of the integrin CD103 which binds E-cadherin on epithelial cells [24] was also up-regulated on protected Tet^+ CD8 T cells, but was not by labeled Tet^+ cells in the lung or Tet^+ memory CD8 T cells in the spleen (either protected or labeld) (Figure 5d). The exclusive expression of CD69 and CD103 by protected but not labeled flu-specific CD8 T cells also indicate that the protected CD8 T cell subset exhibits key features of lung T_{RM}. Taken together with the quantitative analyses in Figure 5c, the lack of CD69 and CD103 expression on labeled and splenic Tet^+ CD8 T cells indicates that the majority of total influenza-specific memory CD8 T cells are circulating.

Lung niches for T_{RM} are independent of lymphoid stores

The longterm maintenance of lung T_{RM} enriched for influenza specificities in a spatially segregated niche, suggested that they could be independently maintained distinct from circulating and lymphoid populations. To test this hypothesis, we treated flu-memory mice with a stable population of lung T_{RM} with the sphinogosine-1-phosphate agonist FTY720 [25, 26] which blocks lymphocyte egress from lymph nodes to determine the resultant effect on the maintenance of lung CD4 and CD8 T_{RM}. Short-term FTY720 treatment of flu-memory mice (40 days post-infection) resulted in >90% reduction in the frequency and number of labeled CD4 and CD8 T cells in the lung, compared to control-treated flu-memory mice (Figure 6a, b). Correspondingly, the frequency of protected T cells increased in FTY720-treated compared to control flu-memory mice; however, there was no difference in the total number of protected T cells in the lungs of treated and control mice (Figure 6a, b, top row), indicating maintenance of lung T_{RM} in the absence of lymphocyte sequestration. Moreover, influenza-specific Tet^+ CD8 lung T_{RM} were likewise maintained in FTY720-treated mice (Figure 6b, lower). These results indicate that virus-specific lung T_{RM} are non-circulating and do not require replenishment from lymphoid populations for their persistence and stability *in situ*.

Compartmentalization of influenza-specific T_{RM} in human lung

Our results in mice indicated a biased compartmentalization of $CD69^+$, influenza-specific memory T cells in a specific niche of the lung, distinct from CD69-negative, circulating T cells that are found in the lung and spleen, but are not resident there. We investigated whether a similar phenomenon was observed in humans. Spleen and lung tissue from individual $HLA\text{-}A2^+$ organs donors were analyzed for the presence of CD8 T cells specific for influenza or cytomegalovirus (CMV) as a representative virus that is not specific for the respiratory tract, using dextramer reagents (see methods). An increased proportion of influenza-specific CD8 T cells was observed in lungs compared to spleen of the same donor, while the proportion of CMV-specific CD8 T cells was similar in both lung and spleen (Figure 7). Importantly, the majority of influenza-specific CD8 T cells in the lung were $CD69^+$, indicating a T_{RM} phenotype, while those in the spleen were predominantly CD69-negative indicating a circulating population (Figure 7a). This increased CD69 expression of flu-specific CD8 T cells in lung compared to spleen was observed in multiple donors analyzed (Figure 7b), analogous to our results in flu-memory mice (Figure 5d). By contrast, CMV-specific CD8 T cells in lung and spleen exhibited comparable CD69 expression with 40–50% $CD69^+$ in both tissues from multiple donors (Figure 7b), indicating that circulating and resident memory populations may be generated from CMV infection. These results suggest that distinct viral pathogens can differentially promote the generation of T_{RM} in specific sites, with flu biasing toward lung T_{RM} generation and CMV infection generating comparable lymphoid and lung T_{RM}.

DISCUSSION

The extent to which T cell responses to virus infection are compartmentalized and whether they develop and/or preferentially persist at the infection site is not well understood. Here, we reveal new insights into how memory T cells are generated and maintained in the lung following respiratory infection with influenza virus. We demonstrate that the expansion and contraction of effector cells and persistence of memory T cells occurs in spatially-defined niches in the lung and are distinct from memory T cells in lymphoid tissues or spleen. Memory T cells in this protected niche were enriched for influenza-specific memory CD4 and CD8 T cells, exhibited upregulation of CD69 and CD11a, did not circulate, and were maintained independent of lymphoid stores—indicating that they represent a new tissue-resident memory subset (T_{RM}). Compartmentalization of influenza-specific memory T cells as lung T_{RM} was also observed in humans, with flu-specific $CD69^+$ memory CD8 T cells enriched in lung compared to spleen from the same individual, and compared to memory CD8 T cells specific for a systemic virus. Together, our findings reveal a precise spatial organization virus-specific T cell memory into circulating and T_{RM} subsets, with the relative proportion of each determined by the site of initial pathogen infection.

We demonstrate the existence of both resident and transient, circulating populations of T cells in the lungs using an *in vivo* antibody labeling approach which delineated T cells subsets that were labeled and protected from IV Ab. Although lung T cells were isolated from tissues perfused extensively to remove all visible traces of blood, and digested to liberate lymphocyte populations as done previously [5, 10, 21, 27], over 90% of T cells in lungs

of naïve mice were accessible to circulation. This labeled population comprised both naïve and memory subsets and disappeared rapidly when T cell egress from lymphoid tissue was blocked, suggesting an equilibrium between lymphoid and circulating lung T cells. By contrast, protected T cells were significantly present only in mice previously infected with influenza, had an effector-memory phenotype, were localized in clusters around airways and maintained independent of circulation and lymphoid egress. Previous studies have suggested that T_{EM} in lungs and other non-lymphoid tissues are replenished during homeostasis from lymphoid stores, and central memory (T_{CM}) subsets [28–30]. However, our results demonstrate that lung T_{RM} cells, are not only spatially segregated, but also are maintained independent of lymphoid and circulating memory T cell populations. Moreover, lung T_{RM} did not appear to be organized in lymphoid-like structures as in ectopic bronchus-associated lymphoid tissues (BALT), which can be induced in acute respiratory infection [31, 32]. We therefore propose that lung T_{RM} are terminally differentiated and irreversibly localized to a specific niche for longterm maintenance.

Lung T_{RM}, as defined here, express phenotypic markers associated with T_{RM} in other sites, including CD69 for both CD4 and CD8 T_{RM}, and CD103 for CD8 T_{RM}. CD69 and CD103 are also upregulated in memory CD8 T cells in the intestines and skin of human and mice [15, 33–36], and in subsets of memory CD8 T cells in human lung [36, 37]. CD69 is expressed at early times following T cell receptor (TCR) signaling [38], or in response to proinflammatory cytokines, including Type I IFNs (IFNα and IFNβ), and TNF-α [39, 40]. Because CD69 is not expressed by flu-specific mouse or human memory T cells in spleen or lymph nodes (Figures 2, 5, 7), we propose that lung T_{RM} are perceiving tonic signals via cytokines or TCR ligation that enable them to be maintained *in situ* in the lung. CD69 itself could play a functional role in retention in tissue sites due to reciprocal regulation of S1PR [41]. However, we found that lung T_{RM} were generated and maintained in the protected niche following influenza infection of CD69-deficient mice (data not shown), suggesting that CD69 expression may act as an indicator of factors that govern the active compartmentalization of lung T_{RM}, rather than through direct functional effects.

Our findings that memory T cells specific for influenza were predominantly lung T_{RM} in both mice and humans suggest that the virus itself, including the site of infection and pathogenesis may determine the anatomic distribution and maintenance of memory T cells. Primary T cell responses to viral infection leading to the generation of memory T cells have been chiefly measured by quantitating $Tetramer^+$ T cells in spleen at different timepoints post-infection [42–44]. Here, we were able to follow the process of expansion, contraction and memory formation of CD4 T cells by examining total cell numbers within a specific niche of the lung—in unmanipulated polyclonal mice. Our findings also suggest that systemic pathogens may generate different type of tissue responses compared to respiratory pathogens. Consistent with this idea, Anderson, et al demonstrated that lung CD8 T_{RM} are not generated by systemic infection with LCMV, but could develop if the infection was administered intranasally[20]. Our results showing that a significant proportion of human CMV-specific T cells expressed CD69 in the spleen (contrasting predominant CD69 expression by flu-specific memory T cells in the human lung), suggests that CMV may promote T_{RM} populations in lymphoid tissues. Further analysis of specificities in different

tissues, along with markers of T_{RM} and *in vivo* labeling approaches in the context of diverse virus infections will enable a mapping of how virus-specific T cells are organized in the body.

Tissue compartmentalization of memory T cells may play a role in preserving the integrity of important memory T cell populations, which might otherwise be reduced by attrition within lymphoid tissues. An individual is exposed to multiple diverse viral pathogens over a lifetime, including acute viruses that are cleared by the immune system, chronic, persistent viruses which evade immune attack, and latent viruses which alternate between prolonged quiescent phases and acute infectious ones. Studies in mice infected with multiple viruses have shown that pre-existing memory T cell populations are quantitatively reduced and qualitatively altered in lymphoid organs in the face of infections with unrelated viruses [45, 46], and that chronic infections can impede the development of memory T cells to ongoing infections [47]. The retention of memory T cell populations at in specific niches may prevent loss of virus-specific memory T cells due to competition by newly formed memory T cells, and can also protect essential immune cells from the effects of virus-induced inflammation. This diversification of storage sites for immune memories may therefore be a key mechanism to enable maintenance of memory responses in the context of new or ongoing infections [48].

The identification of specific protective niches for the development and maintenance of memory T cells after respiratory viral infections has important implications for vaccine design. Focusing protective T cell responses at precise sites within tissues where infections occur, would be a key strategy for promoting protective immune responses, that could potentially improve immune efficacy over systemic approaches.

MATERIALS AND METHODS

Mice

BALB/c mice (8–16 weeks of age) (NCI Biological Testing Branch), and C57BL/6 mice (Taconic Farms, Germantown, NY), were maintained under specific pathogen-free conditions at Columbia University Medical Center (CUMC). Infection and maintenance of mice with influenza virus occurred in a Bsl-2 bio-containment facility in the Irving Comprehensive Cancer Center at CUMC. All animal procedures were conducted according to the NIH guidelines for the care and use of laboratory animals, and were approved by the CUMC Institutional Animal Care and use Committee (IACUC).

Reagents

Fluorescently conjugated Abs specific for CD4 (clones Gk1.5, RM4-4 and RM4-5), CD8α (clone 53–6.7), and CD8β (clone 53–5.8), CD44, CD62L, CD69, IFN-γ and CD11a were purchased from BD Pharmingen (San Diego, CA) and eBiosciences (San Diego, CA). FTY720 was purchased from Cayman Chemical Company (Ann Arbor MI). Tetramers specific for influenza $NP_{366–374}$ and $PA_{224–233}$ H-$2D^b$ were generated as described [49]. Fluorescein-labeled lectin from the Cry-Baby Tree, Erythrina crystagalli (ECL)[23], for staining of lung epithelial cells, was purchased from Vector Labs (Burlingame, CA).

Influenza virus infection

Mice were infected intransally with 100–500 $TCID_{50}$ Influenza virus (A/PR/8/34) for sublethal infection as described [4, 5, 50]. Morbidity was monitored by daily weighing and examination.

In vivo antibody labeling and flow cytometry

For *in vivo* antibody labeling, naïve or flu-memory BALB/c or B6 mice were injected intravenously with 2.5μg Alexa Fluor 700-conjugated anti-CD4 antibody (clone RM4-5) or anti-CD8β (Clone 53–5.8), and after 10 minutes, peripheral blood was obtained by cardiac puncture, lungs were rinsed free of blood and residual antibody and were perfused with PBS/500 units heparin, and cells isolated. Isolated lymphocytes were then stained *in vitro* with a different, non-competing clone of anti-CD4 (RM4-4) as described[21] or anti-CD8α antibodies along with antibodies to other surface markers with fluorochrome-conjugated antibodies. Stained cells were analyzed using an LSRII or FACScanto flow cytometer (BD, San Jose CA), and analyzed using with FlowJo software (Tree Star, Inc., Ashland, OR).

Sample preparation for confocal microscopy

Mice were injected intravenously with 2.5μg Alexa fluor 647–conjugated anti-CD4 Ab (clone GK1.5), and after 10 min, the lungs perfused with PBS/heparin via the right ventricle. The trachea was then exposed and partially severed and the lungs inflated with 1ml 3% agarose (at 55°C) using a syringe and a catheter. The trachea was clamped and the lung bathed in cold PBS then removed. 200–400μm sections were prepared from inflated lung lobes using a Krumdieck Tissue Slicer. Tissue slices were first treated with endogenous streptavidin/biotin-blocking reagents (Life Technologies) then stained with biotin conjugated anti-collagen I mAb (Rockland Immunochemicals Inc, Gilbertsville PA) followed by streptavidin conjugated Dylight 488 (Abcam, Cambridge MA), fluorescein-labeled ECL lectin (Vector Labs), PE conjugated anti-CD4 mAb (clone GK1.5) or PE-conjugated anti CD69. Images were acquired using a Zeiss LSM 700 Laser Scanning Microscope (Thornwood, NY).

Human tissue acquisition and cell isolation

Lung and spleen tissues were obtained from research consented organs donors through an established research protocol and MTA with the New York Organ Donor Network, as previously described [36]. Because tissues were obtained from deceased (and not living) individuals, the study does not qualify as human subjects research, as confirmed by the Columbia University IRB. T lymphocytes were isolated from digested and processed tissues as described [36] and stained with antibodies specific for human CD3, CD8, CD45RO, CD69, and CD19 in conjunction with Dextramer reagents HLA-A*0201(GILGFVFTL)/PE Flu MP and HLA-A*0201(NLVPMVATV)/APC CMV pp65 (Immundex, Copenhagen, Denmark) and analyzed by flow cytometry as above.

Statistics

Results are expressed as the mean value from individual groups +/− SEM unless otherwise designated, indicated by error bars. Significance between experimental groups was determined by two-way ANOVA, assuming a normal distribution for all groups.

Supplementary Material

Refer to Web version on PubMed Central for supplementary material.

Acknowledgments

We wish to thank Philip Camp for help with influenza infections and mouse breeding, Masa Kubota for obtaining human donor tissues, and Drs. Lauren Cohn (Yale University) and Megan Sykes (Columbia University) for critical reading of this manuscript. This work was supported by NIH grants U19AI083022 awarded to D.L.F. and E.J.W. D.L. T. was supported by a Parker Francis Family Foundation Fellowship. Kara L. Bickham was supported by a re-entry supplement to AI083022.

References

1. Doherty PC, Turner SJ, Webby RG, Thomas PG. Influenza and the challenge for immunology. Nat Immunol. 2006; 7:449–455. [PubMed: 16622432]
2. Boyden AW, Legge KL, Waldschmidt TJ. Pulmonary infection with influenza A virus induces site-specific germinal center and T follicular helper cell responses. PLoS One. 2012; 7:e40733. [PubMed: 22792401]
3. Marshall DR, et al. Measuring the diaspora for virus-specific CD8+ T cells. Proc Natl Acad Sci U S A. 2001; 98:6313–6318. [PubMed: 11344265]
4. Teijaro JR, et al. Costimulation modulation uncouples protection from immunopathology in memory T cell responses to influenza virus. J Immunol. 2009; 182:6834–6843. [PubMed: 19454679]
5. Teijaro JR, Verhoeven D, Page CA, Turner D, Farber DL. Memory CD4 T cells direct protective responses to influenza virus in the lungs through helper-independent mechanisms. J Virol. 2010; 84:9217–9226. [PubMed: 20592069]
6. Lee LY, et al. Memory T cells established by seasonal human influenza A infection cross-react with avian influenza A (H5N1) in healthy individuals. J Clin Invest. 2008
7. Roti M, et al. Healthy Human Subjects Have CD4+ T Cells Directed against H5N1 Influenza Virus. J Immunol. 2008; 180:1758–1768. [PubMed: 18209073]
8. Wherry EJ, et al. Lineage relationship and protective immunity of memory CD8 T cell subsets. Nat Immunol. 2003; 4:225–234. [PubMed: 12563257]
9. Woodland DL, Kohlmeier JE. Migration, maintenance and recall of memory T cells in peripheral tissues. Nat Rev Immunol. 2009; 9:153–161. [PubMed: 19240755]
10. Masopust D, Vezys V, Marzo AL, Lefrancois L. Preferential localization of effector memory cells in nonlymphoid tissue. Science. 2001; 291:2413–2417. [PubMed: 11264538]
11. Masopust D, et al. Activated primary and memory CD8 T cells migrate to nonlymphoid tissues regardless of site of activation or tissue of origin. J Immunol. 2004; 172:4875–4882. [PubMed: 15067066]
12. Bevan MJ. Memory T cells as an occupying force. Eur J Immunol. 2011; 41:1192–1195. [PubMed: 21469134]
13. Mueller SN, Gebhardt T, Carbone FR, Heath WR. Memory T cell subsets, migration patterns, and tissue residence. Annu Rev Immunol. 2013; 31:137–161. [PubMed: 23215646]
14. Masopust D, Picker LJ. Hidden memories: frontline memory T cells and early pathogen interception. J Immunol. 2012; 188:5811–5817. [PubMed: 22675215]
15. Jiang X, et al. Skin infection generates non-migratory memory CD8+ TRM cells providing global skin immunity. Nature. 2012; 483:227–231. [PubMed: 22388819]

16. Wakim LM, Woodward-Davis A, Bevan MJ. Memory T cells persisting within the brain after local infection show functional adaptations to their tissue of residence. Proc Natl Acad Sci U S A. 2010; 107:17872–17879. [PubMed: 20923878]
17. Masopust D, et al. Dynamic T cell migration program provides resident memory within intestinal epithelium. J Exp Med. 2010; 207:553–564. [PubMed: 20156972]
18. Shin H, Iwasaki A. A vaccine strategy that protects against genital herpes by establishing local memory T cells. Nature. 2012; 491:463–467. [PubMed: 23075848]
19. Mackay LK, et al. Long-lived epithelial immunity by tissue-resident memory T (TRM) cells in the absence of persisting local antigen presentation. Proc Natl Acad Sci U S A. 2012; 109:7037–7042. [PubMed: 22509047]
20. Anderson KG, et al. Cutting edge: intravascular staining redefines lung CD8 T cell responses. J Immunol. 2012; 189:2702–2706. [PubMed: 22896631]
21. Teijaro JR, et al. Cutting edge: tissue-retentive lung memory CD4 T cells mediate optimal protection to respiratory virus infection. J Immunol. 2011; 187:5510–5514. [PubMed: 22058417]
22. Wakim LM, Gupta N, Mintern JD, Villadangos JA. Enhanced survival of lung tissue-resident memory CD8(+) T cells during infection with influenza virus due to selective expression of IFITM3. Nat Immunol. 2013; 14:238–245. [PubMed: 23354485]
23. Helms MN, et al. Dopamine activates amiloride-sensitive sodium channels in alveolar type I cells in lung slice preparations. Am J Physiol Lung Cell Mol Physiol. 2006; 291:L610–618. [PubMed: 16679376]
24. Strauch UG, et al. Integrin alpha E(CD103)beta 7 mediates adhesion to intestinal microvascular endothelial cell lines via an E-cadherin-independent interaction. J Immunol. 2001; 166:3506–3514. [PubMed: 11207310]
25. Brinkmann V, et al. The immune modulator FTY720 targets sphingosine 1-phosphate receptors. J Biol Chem. 2002; 277:21453–21457. [PubMed: 11967257]
26. Brinkmann V, Lynch KR. FTY720: targeting G-protein-coupled receptors for sphingosine 1-phosphate in transplantation and autoimmunity. Curr Opin Immunol. 2002; 14:569–575. [PubMed: 12183155]
27. Bingaman AW, et al. Novel phenotypes and migratory properties distinguish memory CD4 T cell subsets in lymphoid and lung tissue. Eur J Immunol. 2005; 35:3173–3186. [PubMed: 16220537]
28. Kohlmeier JE, Woodland DL. Memory T cell recruitment to the lung airways. Curr Opin Immunol. 2006; 18:357–362. [PubMed: 16616475]
29. Marzo AL, Yagita H, Lefrancois L. Cutting edge: migration to nonlymphoid tissues results in functional conversion of central to effector memory CD8 T cells. J Immunol. 2007; 179:36–40. [PubMed: 17579018]
30. Sallusto F, Geginat J, Lanzavecchia A. Central memory and effector memory T cell subsets: function, generation, and maintenance. Annu Rev Immunol. 2004; 22:745–763. [PubMed: 15032595]
31. Moyron-Quiroz JE, et al. Role of inducible bronchus associated lymphoid tissue (iBALT) in respiratory immunity. Nat Med. 2004; 10:927–934. [PubMed: 15311275]
32. Randall TD. Bronchus-associated lymphoid tissue (BALT) structure and function. Adv Immunol. 2010; 107:187–241. [PubMed: 21034975]
33. Liu L, et al. Epidermal injury and infection during poxvirus immunization is crucial for the generation of highly protective T cell-mediated immunity. Nat Med. 2010; 16:224–227. [PubMed: 20081864]
34. Masopust D, Vezys V, Wherry EJ, Barber DL, Ahmed R. Cutting edge: gut microenvironment promotes differentiation of a unique memory CD8 T cell population. J Immunol. 2006; 176:2079–2083. [PubMed: 16455963]
35. Casey KA, et al. Antigen-Independent Differentiation and Maintenance of Effector-like Resident Memory T Cells in Tissues. J Immunol. 2012; 188:4866–4875. [PubMed: 22504644]
36. Sathaliyawala T, et al. Distribution and compartmentalization of human circulating and tissue-resident memory T cell subsets. Immunity. 2013; 38:187–197. [PubMed: 23260195]
37. Purwar R, et al. Resident memory T cells (T(RM)) are abundant in human lung: diversity, function, and antigen specificity. PLoS One. 2011; 6:e16245. [PubMed: 21298112]

38. Ziegler SF, Ramsdell F, Alderson MR. The activation antigen CD69. Stem Cells. 1994; 12:456–465. [PubMed: 7804122]
39. Freeman BE, Hammarlund E, Raue HP, Slifka MK. Regulation of innate CD8+ T-cell activation mediated by cytokines. Proc Natl Acad Sci U S A. 2012; 109:9971–9976. [PubMed: 22665806]
40. Sun S, Zhang X, Tough DF, Sprent J. Type I interferon-mediated stimulation of T cells by CpG DNA. J Exp Med. 1998; 188:2335–2342. [PubMed: 9858519]
41. Matloubian M, et al. Lymphocyte egress from thymus and peripheral lymphoid organs is dependent on S1P receptor 1. Nature. 2004; 427:355–360. [PubMed: 14737169]
42. Williams MA, Ravkov EV, Bevan MJ. Rapid culling of the CD4+ T cell repertoire in the transition from effector to memory. Immunity. 2008; 28:533–545. [PubMed: 18356084]
43. Murali-Krishna K, et al. Counting antigen-specific CD8 T cells: a reevaluation of bystander activation during viral infection. Immunity. 1998; 8:177–187. [PubMed: 9491999]
44. Kaech SM, Wherry EJ. Heterogeneity and cell-fate decisions in effector and memory CD8+ T cell differentiation during viral infection. Immunity. 2007; 27:393–405. [PubMed: 17892848]
45. Selin LK, et al. Attrition of T cell memory: selective loss of LCMV epitope-specific memory CD8 T cells following infections with heterologous viruses. Immunity. 1999; 11:733–742. [PubMed: 10626895]
46. McNally JM, et al. Attrition of bystander CD8 T cells during virus-induced T-cell and interferon responses. J Virol. 2001; 75:5965–5976. [PubMed: 11390598]
47. Stelekati E, Wherry EJ. Chronic bystander infections and immunity to unrelated antigens. Cell Host Microbe. 2012; 12:458–469. [PubMed: 23084915]
48. Odumade OA, et al. Primary Epstein-Barr virus infection does not erode preexisting CD8(+) T cell memory in humans. J Exp Med. 2012; 209:471–478. [PubMed: 22393125]
49. Altman JD, et al. Phenotypic analysis of antigen-specific T lymphocytes. Science. 1996; 274:94–96. [PubMed: 8810254]
50. Verhoeven D, Teijaro JR, Farber DL. Pulse-oximetry accurately predicts lung pathology and the immune response during influenza infection. Virology. 2009; 390:151–156. [PubMed: 19493556]

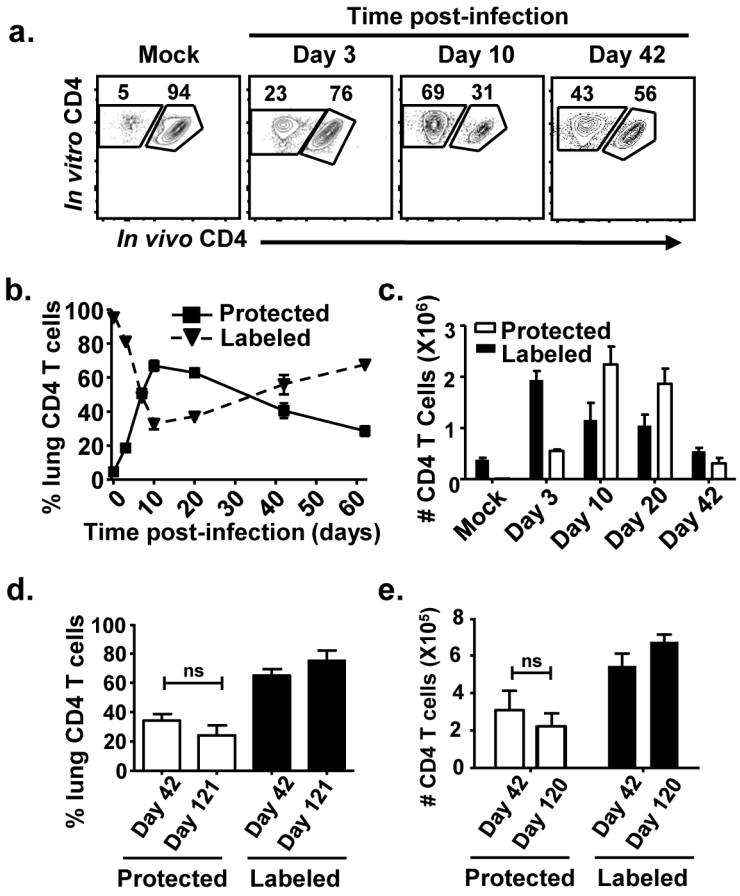

Figure 1. Influenza infection generates an increased proportion of lung CD4 T cells which are protected from *IN VIVO* antibody labeling

(a) Flow cytometric analysis of lung CD4 T cells labeled by or protected from intravenously administered fluorescent anti-CD4 antibody at 3, 10 and 42 days following influenza infection. **(b)** Frequency of lung CD4 T cells that are labeled by or protected from *in vivo* CD4 labeling. Graph displays means ± SEM (n= 6 mice per time point compiled from 2 independent experiments; representative of 5 experiments). **(c)** Absolute numbers of labeled and protected CD4 T cells in the lung throughout the course of influenza virus infection. These results are expressed as means from 3 mice per group and are representative of 3 experiments. **(d)** Frequency of lung CD4 T cells that are labeled by or protected from *in vivo* anti-CD4 labeling at 42 and 121 days post influenza virus infection. (n= 3 mice per group, **ns P> 0.05;** Representative of 3 independent experiments) **(e)** Absolute numbers of protected and labeled CD4 T cells in the lung at 42 and 120 days post infection. (n= 3 mice per group, **ns P> 0.05;** Representative of 3 independent experiments)

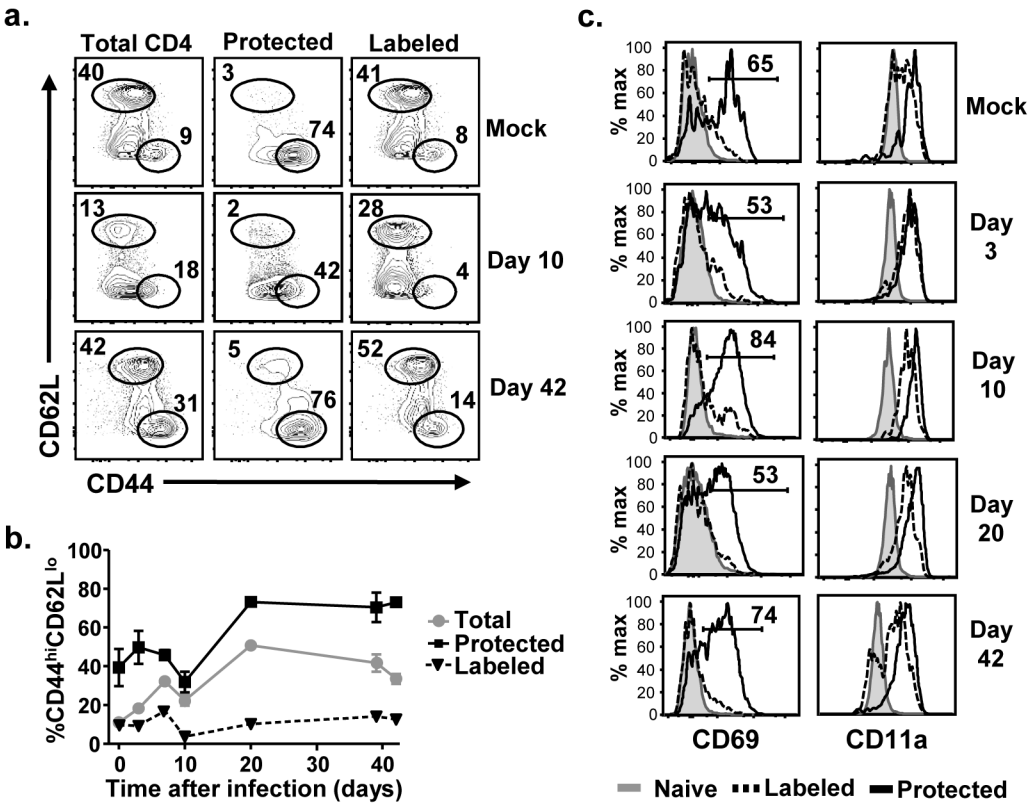

Figure 2. Differential phenotype and subset composition of protected and labeled lung CD4 T cell subsets

(a) Flow cytometric analysis of lung CD4 T cells stratified into total, labeled and protected fractions, from naïve and flu-infected mice days 10 and 42 post-infection. Plots show the percent of cells with naïve ($CD44^{lo}CD62^{hi}$) and effector/memory ($CD44^{hi}CD62L^{lo}$) phenotypes **(b)** Graph shows frequency (mean± SEM) of effector/memory ($CD44^{hi}CD62L^{lo}$) cells in total, protected and labeled lung CD4 T cell subsets (n= 3–6 mice per time point compiled from independent experiments; Representative of >3 experiments). **(c)** CD69 (left) and CD11a (right) expression by naïve, labeled memory, and protected memory CD4 T cells from the lung at various times following influenza infection.

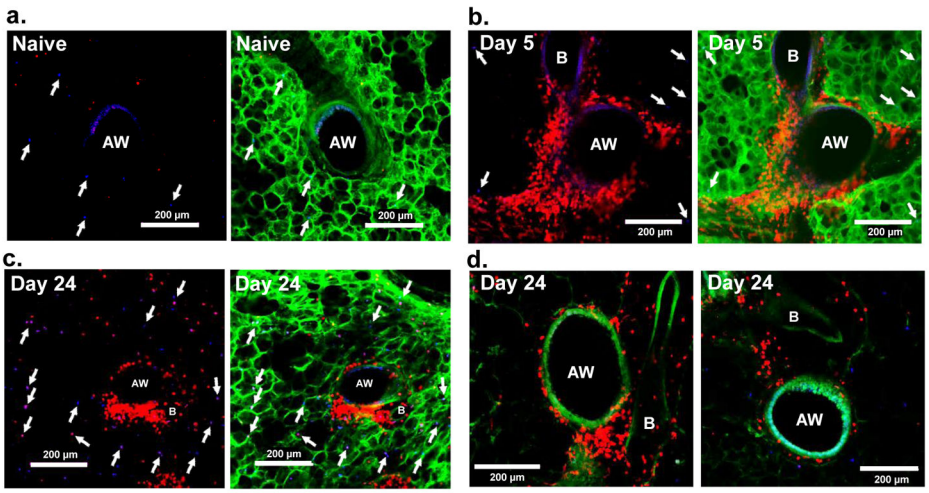

Figure 3. Distinct localization of labeled and protected memory CD4 T cells in niches of the lungs

Naïve and Flu-infected mice were *in vivo* labeled with anti-CD4 MAb (blue) and lung slices stained with a second clone of anti-CD4 mAb (red), anti-collagen Type I mAb (green) and ECL (green). Representative images show the localization of *in vivo* labeled (Blue or blue-violet) and Protected (red) CD4 T cells in the lungs of naïve mice **(a)**, and influenza-infected mice 5 days **(b)** and 24 days **(c)** post infection showing airways (AW) and major blood vessels (B) **(d)** Representative images showing *in vivo* labeled and Protected CD4 T cells and collagen-stained airways (green) (no ECL staining). Images are representative of >20 mice analyzed from independent influenza infections.

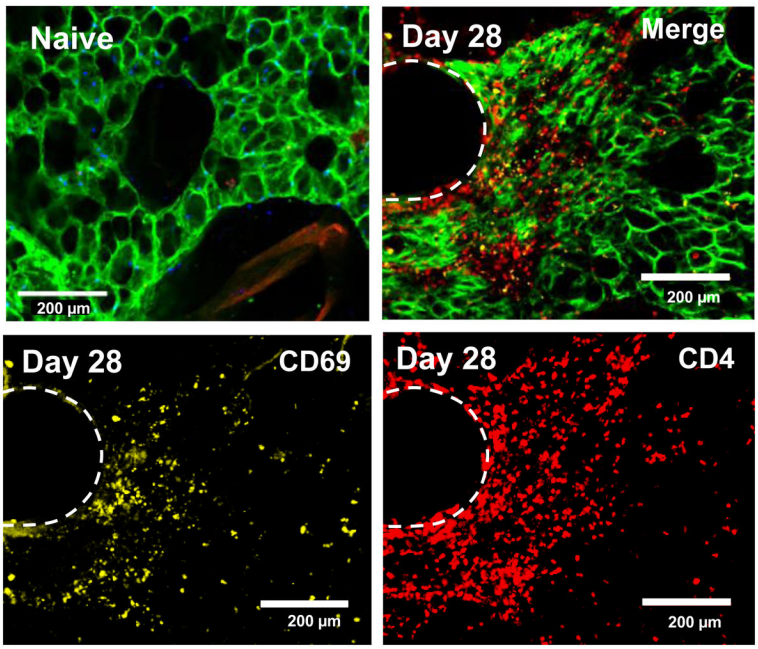

Figure 4. CD69-expressing CD4 T cells define spatially distinct niches of resident cells within the lung

CD69 expression (yellow) by CD4 T_{RM} cells organized in niches around airways 28 days following flu infection. Naïve lung shows negligible CD69 expression (Upper left). (Images are representative of 4 independent experiments)

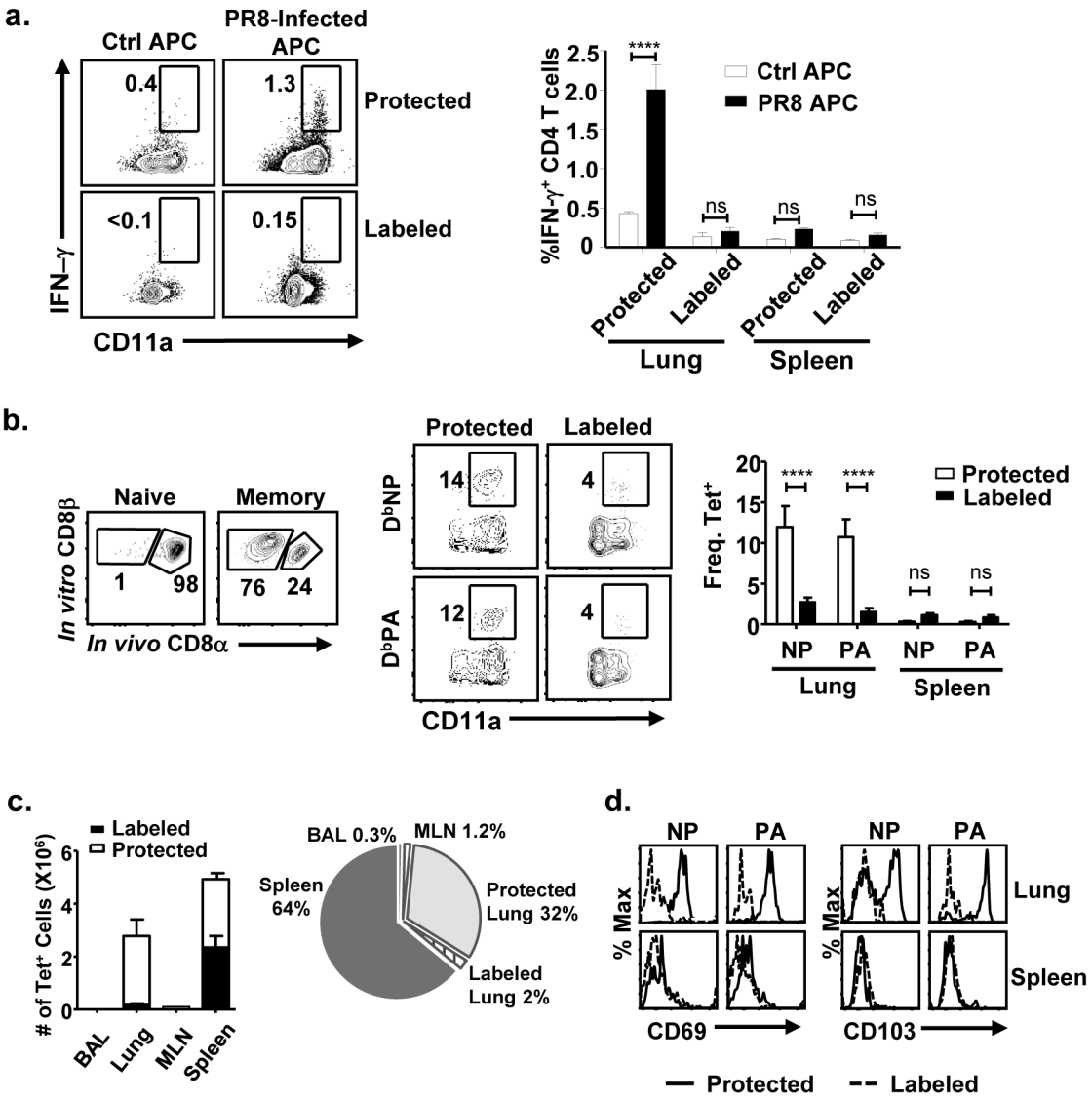

Figure 5. Influenza-specific memory CD4 T cells are localized exclusively in the protected niche of the lung

(a) Left : Flow cytometric analysis of IFN-γ expression by labeled and protected lung CD4 T cells from influenza memory mice after *in vitro* stimulation with PR8 influenza infected antigen presenting cells. Right : Percent IFN-γ^+ CD4 T cells in the labeled and protected lung subsets and total spleen CD4 T cells. Graph displays means ± SEM (n=5 mice per time point) Representative of 3 independent experiments **** **P< 0.0001, ns P> 0.05. (b)** Left: Flow cytometric analysis showing lung CD8 T cells labeled by or protected from intravenously administered fluorescent anti-CD8α in the lungs of naïve or flu –infected mice, and the frequency of labeled and protected lung CD8 T cells that are stained with $NP_{366–374}$ and $PA_{224–233}$ H-2D^b tetramers (mean ± SEM). Right: Frequency of labeled and protected CD8 T cells in the lung and spleen that are specific for $NP_{366–374}$ and $PA_{224–233}$ H-2D^b tetramers (mean ± SEM) (n=6 mice per group from two independent experiments. **** P< 0.0001, ns P> 0.05). **(c)** *In vivo* labeling of CD8 T cells was performed in Flu-

memory mice at day 133 post infection and the number of CD8 T cells that are specific for $NP_{366–374}$ and $PA_{224–233}$ H-$2D^b$ tetramers in the BAL fluid, lung, MLN and spleen calculated. Left: Graph shows the number of labeled and protected Tet^+ CD8 T cells in the various sites (n=4). Right: Pie charts show the relative distribution of Tet^+ CD8 T cells, averaged from four mice. **(d)** Representative histograms showing CD69 and CD103 expression by labeled and protected lung flu-tetramer-positive (Tet^+) and Tet-negative CD8 T cells in the lung and spleen of flu-memory mice. Results are representative of 6 independent experiments.

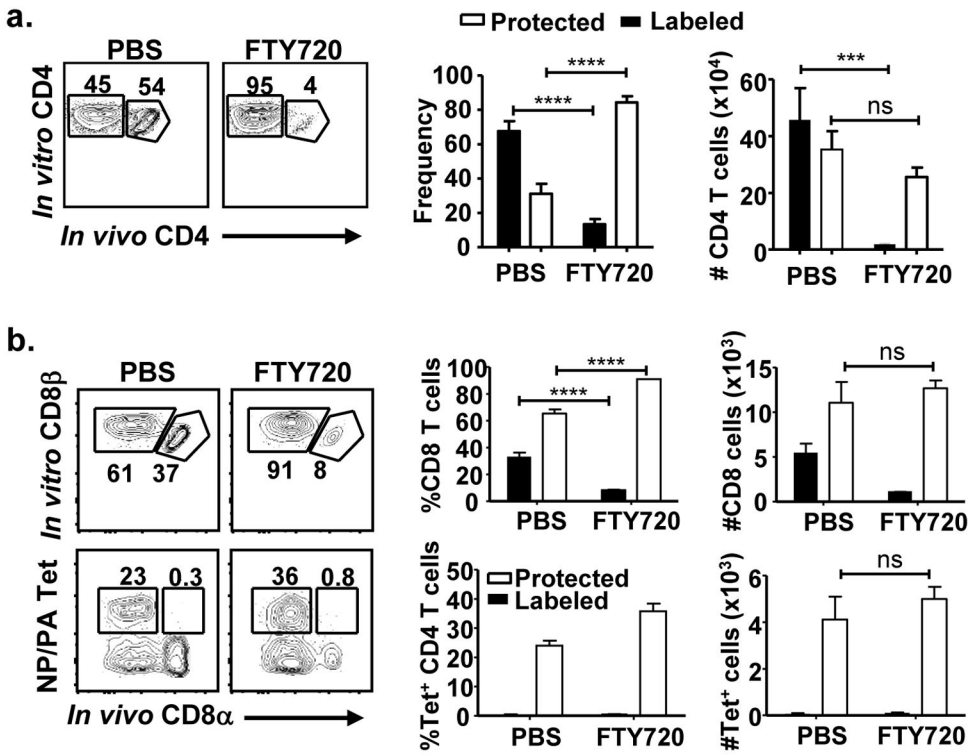

Figure 6. Lung T_{RM} cells in the protected niche are maintained independent of lymphoid stores

In vivo anti-CD4 or CD8 antibodies were administered to Flu-memory mice treated with FTY720 (or PBS) for three consecutive days. **(a)** Left: Flow cytometric analysis of lung CD4 T cells labeled by or protected from IV anti-CD4 antibody from FTY720- and PBS-treated mice. Right: Frequency and absolute numbers of labeled and protected CD4 T cells in FTY720- PBS-treated mice. Graph displays means ± SEM (n=3–4 mice per group) n=7 mice per group from two independent experiments, representative of 3 experiments. **** $P < 0.0001$, ns $P > 0.05$. **(b)** Left: Flow cytometric analysis of lung CD8 T cells labeled by or protected from IV fluorescent anti-CD8 antibody in FTY720- and PBS-treated mice. Lower plots show proportion of $NP_{366–374}$ and $PA_{224–233}$ H-$2D^b$ $tetramer^+$ CD8 T cells within protected and labeled lung CD8 T cells. **(c)** Percentage and absolute numbers of labeled and protected CD8 T cells (upper graphs) and $Tetramer^+$ CD8 T cells (lower graphs) in FTY720- or PBS-treated mice. Graph displays means ± SEM (n=3 mice per group, representative of 3 experiments).

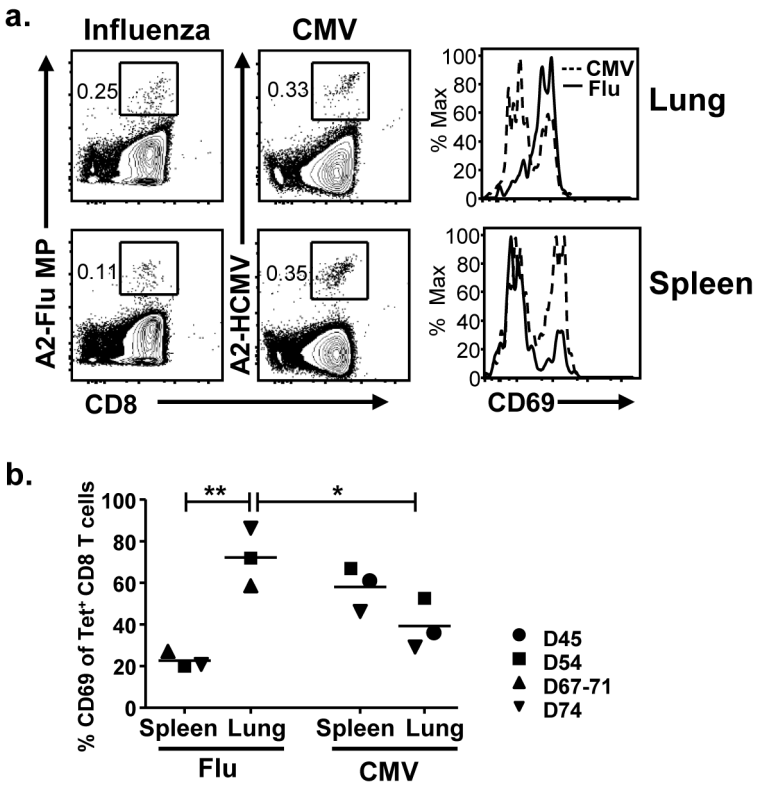

Figure 7. Compartmentalization of human influenza-specific T_{RM} in the lung

T cells were isolated from lung and spleen tissues isolated from individual organs donors (HLA-A2^{+}) as described [36], stained for T cells markers and influenza or CMV-specific dextramer reagents (see methods) and analyzed by flow cytometry. **(a)** Left: Frequency of influenza and CMV-specific CD8 T cells in lungs and spleen of a 48 yr old donor with positive CMV serology. Right: CD69 expression by flu- and CMV-specific CD8 T cells in each tissue site. **(b)** CD69 expression by flu- and CMV-specific CD8 T cells in the lungs and spleens of multiple human donors. (Donors: D45, 37 y.o. male; D54, 33 y.o. male; D71, 47 y.o. female; D74, 48 y.o. female). (* P< 0.05, ** P<0.001 2-way ANOVA)